



Pressure-induced change in magnetic and transport properties of layered $(\text{La}_{0.6}\text{Nd}_{0.4})_{1.2}\text{Sr}_{1.8}\text{Mn}_2\text{O}_7$

K.V. Kamenev*, M.R. Lees, G. Balakrishnan, C.D. Dewhurst, D.M^ck. Paul

Department of Physics, University of Warwick, Coventry CV4 7AL, UK

Abstract

We report the results of transport measurements on a single crystal of layered $(\text{La}_{0.6}\text{Nd}_{0.4})_{1.2}\text{Sr}_{1.8}\text{Mn}_2\text{O}_7$ manganese oxide. We find that the low-temperature magnetic order can be switched from easy-plane antiferromagnetic to easy-axis ferromagnetic by the application of pressures higher than 8 kbar. This behavior is explained in terms of the competition between super and double exchange in the Mn–O network. © 1999 Elsevier Science B.V. All rights reserved.

PACS: 61.50.Ks; 75.30.Et; 75.30.Vn

Keywords: Magnetism; Transport properties; Superexchange; Double exchange

1. Introduction

The layered $(\text{La}_{0.6}\text{Nd}_{0.4})_{1.2}\text{Sr}_{1.8}\text{Mn}_2\text{O}_7$ material belongs to the series of perovskite oxides with the general formula $(\text{R}_{1-x}\text{A}_x)_{n+1}\text{Mn}_n\text{O}_{3n+1}$ where R is a rare-earth ion and A is a divalent cation. These materials have recently attracted a great deal of interest due to the colossal negative magnetoresistance (CMR) occurring near the magnetic phase transition [1,2]. The electronic configuration of the 3d shell in Mn atoms consists of a t_{2g} triplet and an e_g doublet. A dumbbell $3d_{x^2-y^2}$ or $3d_{z^2}$ of the e_g orbital is aligned along the Mn–O bond, while the electronic density in any of the $3d_{xy}$, $3d_{xz}$, or $3d_{yz}$ orbitals is concentrated between the bonds.

Oxygen's 2p electronic shell also has two types of orbitals: p_σ – along the bond and p_π – perpendicular to the bond. From this we can conclude that the p_σ orbital is orthogonal to the t_{2g} orbital, while the p_π is orthogonal to the e_g . Electron transfer can only take place between non-orthogonal orbitals, i.e. between a p_σ and an e_g orbitals as well as between the p_π and t_{2g} orbitals. Since the orbital overlap along the bond is greater and because the t_{2g} electrons are more localized than the e_g electrons due to the lower energy of the triplet with respect to the doublet, p_σ – e_g transfer is stronger than p_π – t_{2g} .

In undoped manganese oxides ($x = 0$) all the Mn ions have four 3d-electrons of which three occupy the t_{2g} triplet and the other one occupies an e_g orbit. The Pauli exclusion principle constrains the number of electrons of each spin in the p_σ – e_g and p_π – t_{2g} overlap regions to one. Therefore, only antiparallel

* Corresponding author. Fax: +44-1203-692016; e-mail: k.kamenev@warwick.ac.uk.

coupling of spins is allowed on both ends of the cation–anion–cation bond giving rise to an antiferromagnetic (AF) order of the magnetic moments. This AF coupling is called superexchange [3]. When a rare-earth ion R is substituted by a divalent ion, A, in $(R_{1-x}A_x)_{n+1}Mn_nO_{3n+1}$ ($x > 0$), some Mn^{3+} ions become Mn^{4+} ions after transferring their e_g electron to the divalent ions. In this case a p_σ orbital overlaps with an empty e_g orbital on one side of the $Mn^{3+} - O^{2-} - Mn^{4+}$ bond. Therefore, the transferred p_σ orbitals are antiparallel to the cation spin on one side and parallel on the other giving ferromagnetic (FM) coupling. The $p_\pi-t_{2g}$ overlap still favours AF coupling but it is now weaker than the FM coupling from $p_\sigma-e_g$ overlap and the net interaction is FM. This FM coupling between the Mn atoms of different valence is called *double exchange* [4].

It is the interplay between the double exchange and superexchange that defines the long-range magnetic order in doped manganites. This interplay can be controlled by either doping level, which changes the Mn^{3+}/Mn^{4+} ratio or pressure which effects the overlap between cation and anion orbitals in the Mn–O network. Parallel alignment of the magnetic moments on the manganese sites can also be achieved by the application of an external magnetic field. The application of pressure is the best probe for the role of such interactions. It neither changes the number of charge carriers in the material (as doping does), nor does it introduce a preferred orientation for the magnetic moments (as a magnetic field does).

We have chosen to study a sample with $z = 0.4$ from the series of $(La_{1-z}Nd_z)_{1.2}Sr_{1.8}Mn_2O_7$ manganites for the following reason. Our recent neutron diffraction experiments have shown that at ambient pressure $(La_{0.6}Nd_{0.4})_{1.2}Sr_{1.8}Mn_2O_7$ is an “easy-plane” antiferromagnet below $T \sim 50$ K [5]. In a sample of this composition parallel alignment of the magnetic moments can be achieved in an applied magnetic field of greater than 1 T [6]. The aim of the present study is to reach the PM–FM phase transition by application of high pressure and to find out how the external pressure influences the $p_\sigma-e_g$ and $p_\pi-t_{2g}$ cation–anion interactions.

2. Experimental details

Single crystals of $(La_{0.6}Nd_{0.4})_{1.2}Sr_{1.8}Mn_2O_7$ were grown from polycrystalline rods in an infrared image furnace using the floating-zone method. The electrical resistivity ρ was measured along the ab crystallographic plane using a standard four-point technique. Contacts to the crystal were made on a bar-shaped sample using silver-based epoxy. The pressure measurements were made in a CuBe pressure cell with Fluorinert as a pressure transmitting medium. Pressure, P , and temperature, T , were measured using a calibrated manganin sensor and a Cernox resistor, respectively.

3. Results and discussion

To characterize the material a tiny piece of crystal was ground to a powder and checked with X-ray diffraction. The space group is I4/mmm with the lattice parameters of the tetragonal unit cell being $a = 3.85(7)$ Å and $c = 20.12(9)$ Å. The unit cell ($Z = 2$) is shown in Fig. 1. Manganese atoms occupy the positions at the center of each MnO_6 octahedra, with the octahedra forming the double layers extending along the basal ab plane.

The set of the curves presenting the temperature dependence of ρ for ascending temperature sweeps at several pressures is shown in Fig. 2. It should be noted that because of differences in the thermal expansion coefficients of the pressure transmitting medium and the pressure cell, the pressure inside the cell decreases as the temperature is lowered. The actual pressure at a given temperature can be calculated from the electrical resistivity of the calibrated manganin sensor. The curves in the Fig. 2 are marked according to the clamping pressures of 0, 4.5, 6, 9 and 11 kbar at room temperature.

At ambient pressure the PM–AF phase transition is marked by a sharp drop in the electrical resistivity with the maximum at $T = T_N$. Above and below this peak the resistivity increases with decreasing temperature reflecting the non-metallic nature of the material in both these phases. Nevertheless, the conductivities in the PM and AF phases have different character for their temperature behavior. The high-temperature conduction has

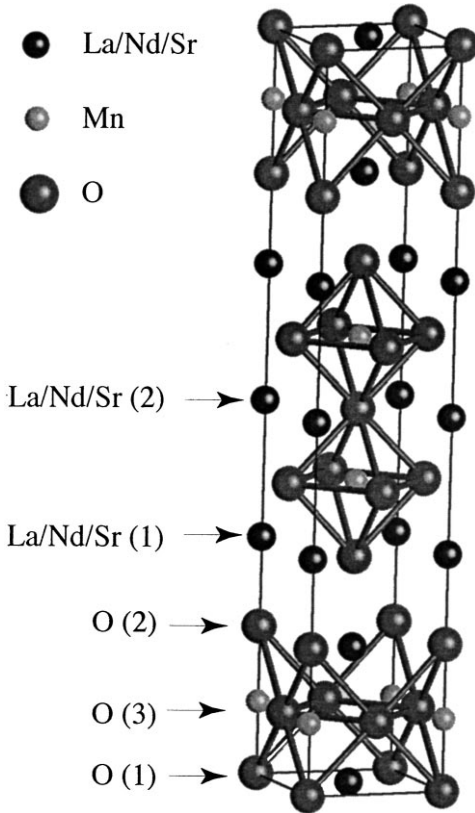


Fig. 1. The crystal structure of $(\text{La}_{0.6}\text{Nd}_{0.4})_{1.2}\text{Sr}_{1.8}\text{Mn}_2\text{O}_7$.

a form similar to that expected for variable-range hopping, i.e. $\ln \rho \propto T^{-1/4}$. However, in the AF phase, the resistivity increases linearly with decreasing temperature. This could be due to an additional contribution to the hopping from the magnetic sub-lattice which polarizes the electrons in the mean field of the ordered magnetic moments on the Mn sites.

Applied pressure increases the Néel temperature at a rate of $dT_N/dP = 1.8 \text{ K/kbar}$, as shown in Fig. 3. The resistivity of the AF phase rapidly decreases with increasing pressure but remains linearly dependent on temperature somewhat below T_N . We can estimate the pressure dependence of the $d\rho/dT$ slope of the resistivity curves measured at different pressures at temperatures below 35 K shown in Fig. 4. The pressure behaviour of the $d\rho/dT$ ratio shows an exponential dependence and

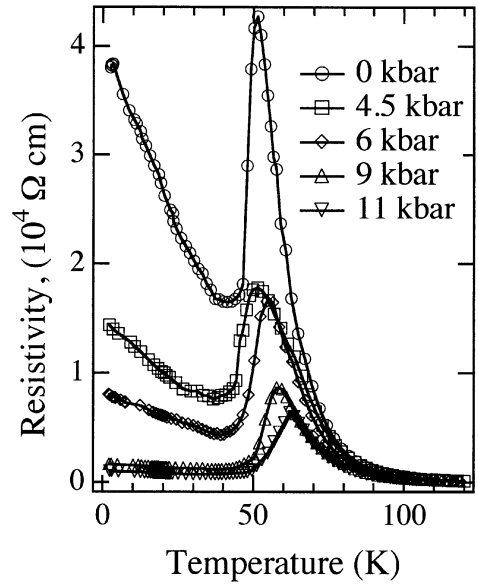


Fig. 2. Temperature dependence of ρ at different pressures.

can be fitted adequately by the expression:

$$d\rho/dT = K_0 + K_1 \exp[-K_2 * P],$$

where $K_0 = -0.5814$, $K_1 = -548.841$, $K_2 = 0.4971$. The exponential decay of the resistivity with pressure at a constant temperature in the AF phase can be explained in the following way. The spin-independent electron transfer integral is proportional to the orbital overlap and so must increase exponentially with decreasing cation–anion–cation separation [7]. As we mentioned above, the increased overlap will greatly enhance the transfer of a p_σ orbital which, in the case of the mixed valence $\text{Mn}^{3+}/\text{Mn}^{4+}$ manganese ions, favors the FM interaction. Superexchange between half-filled t_{2g} orbitals dominates in the AF phase giving a virtual charge transfer and insulating behavior. Double exchange between half-empty and empty e_g orbitals favors real charge transfer and a metallic type of conductivity.

Figs. 2 and 3 demonstrate that at the clamping pressure of 11 kbar (the actual pressure near T_N is 7.9 kbar) the resistivity increases only slightly with decreasing temperature below T_N . This indicates that at low temperatures the stabilization energies of the AF and FM order are almost equal.

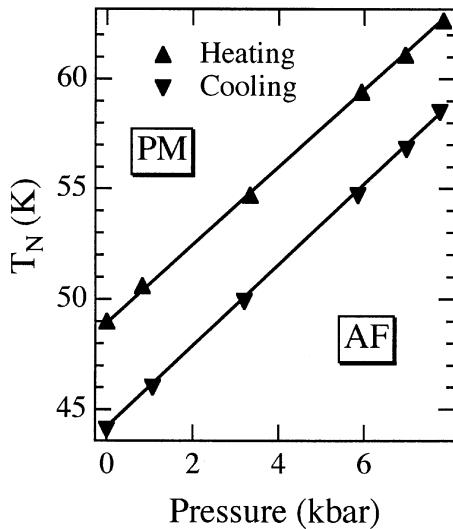


Fig. 3. Pressure–temperature phase diagram of $(\text{La}_{0.6}\text{Nd}_{0.4})_{1.2}\text{Sr}_{1.8}\text{Mn}_2\text{O}_7$.

Unfortunately, the upper pressure limit of the cell does not allow us to go to higher pressures to see the PM–AF phase transition changing into a PM–FM phase transition. Recently, magnetic AC susceptibility has been measured on a sample of the same composition in a diamond anvil cell under pressures of up to 71 kbar. These measurements show that the change from AF to FM order takes place at slightly above 8 kbar [8].

In conclusion, we have studied the pressure dependence of the electrical resistivity of the layered $(\text{La}_{0.6}\text{Nd}_{0.4})_{1.2}\text{Sr}_{1.8}\text{Mn}_2\text{O}_7$ in the vicinity of the Néel temperature. We find that the application of pressure suppresses AF order and favors a ferromagnetic alignment of magnetic moments on the manganese sites, making the sample more metallic

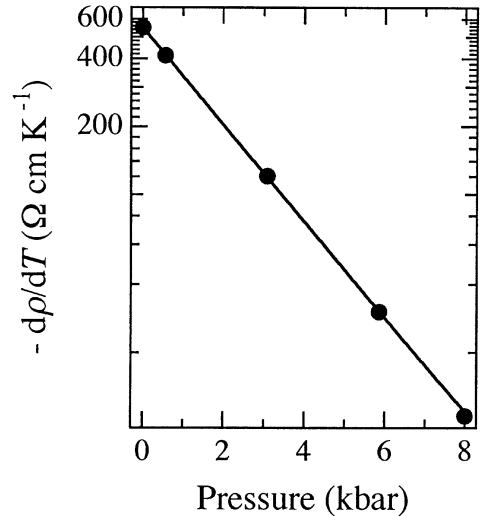


Fig. 4. Pressure dependence of $d\rho/dT$ below T_N ; note the values for $d\rho/dT$ have been multiplied by a factor of -1 in order to plot the data using a logarithmic scale.

below T_N . The results are interpreted in terms of the competition between antiferromagnetic superexchange and ferromagnetic double exchange in a Mn–O network.

References

- [1] Y. Moritomo et al., *Nature* 380 (1996) 141.
- [2] A.P. Ramirez, *J. Phys.: Condens. Matter* 9 (1997) 8171.
- [3] C. Zener, *Phys. Rev.* 82 (1951) 403.
- [4] P.W. Anderson, *Phys. Rev.* 79 (1950) 350.
- [5] K.V. Kamenev et al., to be published.
- [6] Y. Moritomo et al., *Phys. Rev. B* 56 (1997) R7057.
- [7] J.B. Goodenough, in: *Magnetism and the Chemical Bond*, Wiley, New York, 1963.
- [8] V.G. Tissen et al., to be published.